We are IntechOpen, the world's leading publisher of Open Access books Built by scientists, for scientists

6,900
Open access books available

186,000
International authors and editors

200M
Downloads

154
Countries delivered to

Our authors are among the

TOP 1%
most cited scientists

12.2%
Contributors from top 500 universities

CLARIVATE ANALYTICS
BOOK CITATION INDEX
INDEXED

WEB OF SCIENCE™

Selection of our books indexed in the Book Citation Index
in Web of Science™ Core Collection (BKCI)

Interested in publishing with us?
Contact book.department@intechopen.com

Numbers displayed above are based on latest data collected.
For more information visit www.intechopen.com

Novel Predictors for Friction and Wear in Drivetrain Applications

Walter Holweger

Abstract

Reliability in a drivetrain is given by the life of its constituents, e.g., gears, clutches, and bearings. Lubrication contributes to the life cycle, preventing wear, friction, and environmental impacts. As lubricants and their additives are chemicals with an expected reactivity in a tribological contact, it comes to the question how surface fatigue phenomena due to loading may be influenced by the reactivity of functional additives and how this might be embedded in construction guidelines. A very basic study based on an elementary gear test rig presents the result that pitting life of a gear is substantially influenced by the chemical structure of wear-preventing additives. Even under appropriate loading conditions, the lubricant structure comes as a life-limiting factor. A molecular model shows how the release and the approach of the additives toward a surface is essential and related to the reaction processes that occur during the loading.

Keywords: drivetrain, gears, bearings, reliability, pitting, wear, gray staining, life cycle, molecular modeling

1. Introduction

Wear is a central topic in tribology. As a system property, it is defined as a continuous loss of material out of a solid surface, caused by mechanical impact, e.g., contact and relative motion of counterpart such as solids, liquids, or gases [1–6].

As such, wear is not a property of a single component. Drivetrain components (e.g., bearings, gears, clutches, etc.) are constructed due to their life expectation in order to come to a predictive reliability in the life cycle. However, in reality they are exposed to wear processes as an incidental or continuous impact. Hence, it is important to know how the entrance of wear in drivetrain components will influence their life expectations and the reliability of the drivetrain as such.

Within a construction, the expected life is a function of the load capacity of the materials, e.g., their fatigue strength with respect to load cycles and pressure.

As reliability is defined yet by the load capacity of the involved materials due to cyclic stress, the question is about how wear relates to fatigue. In a classical view, fatigue is a matter related to stress-strain properties due to the elastic plastic behavior of the load carrying components. If a pressure with no tangential component acts on moving parts, the fatigue phenomena are given by slow changes of the subsurface microstructure due to phase alterations, migration of interstitial atoms, and dislocations. As tangential forces due to slip are coming up, the fatigue processes moves up toward the surface. However, fatigue phenomena near the surface

will bring up the question at which point fatigue crosses wear and vice versa. While reliability up to now is defined by fatigue properties of the material, the crossing between fatigue and wear, especially those, induced by lubricants is still not solved. Within real applications it might be the case that, due to the operating conditions, fatigue comes to lubricant-induced wear and does not fit with the standard construction guidelines.

We present here a basic study, how fatigue and lubricant-induced wear push each other in a standard gear and bearing test. It comes up that this stimulation is due to the basic behavior of lubricant components, e.g., the reactivity of additives combined with the mechanical loading. As a main and future question of research, it addresses the need of advanced understanding on a molecular scale (10^{-9} m), molecular modeling, and in situ spectrometry to embed them in future construction guidelines.

2. Gear and bearing life in terms of lubricants

Pitting and gray staining in gears and bearings appear as surface features. In a worst case, they may promote a decay in life expectation, due to their progression in time.

Within the traditional view, they are interpreted by the assumption that loading exceeds the load capacity of the material. Consequently the mating parts will get in touch and come to rupture. As such, lubricants as separating media are only seen as a material to avoid this by separating the surfaces due to viscous effects. However, it is well known that lubricants as a matter of their composition will influence the surface load capacity as well (see **Figure 1**) [7, 8] as seen for gears in FZG standard test conditions, using SAE 4320 case-hardened material [7–9].

Figure 2 shows the wear rate by the use of different anti-wear and extreme pressure additives base on the FZG test rig (16) as a function of the pitch line speed:

Same as for gears, bearings are impacted also by wear raising from the composition of a lubricant [10, 11] (see **Figure 3**), using the Schaeffler FE8 test rig as a standard (2100 MPa contact pressure, 80 rpm, 80 h, cylindrical roller bearing, SAE 52100, Martensite):

Within the FZG gear test rig [9, 12–17] (DIN ISO 14635), different lubricants (A, B) differ in wear as a fact of temperature. While oil A shows a decay by raising the temperature, oil B is opposite (see **Figure 4**).

As a result of those studies, reaction layers with different thicknesses under mechanical influence are created. While thick and uncontrolled layers cause early fatigue and wear, thin oxide layers with a strong bonding to the interface cause no wear, same as reported earlier [1, 11]. It is of interest to describe these effects with respect to their chemical structures of the reactive components and how they undergo a transformation of the tribological contact area by creating those layers. Structure property relationship would lead to predictors for wear derived from the chemical structure of a given lubricant.

As a standard the FZG test rig (DIN ISO 14635) as a back-to-back gear test is used (**Figure 5**) [7, 18–20]. The gears, type FZG C-PT, are set in a gearbox, fully lubricated. Cylindrical roller bearings (type NJ406, steel cage) are used for the pinion shaft 1 and cylindrical roller bearings, type NJ308, for the motor shaft. Investigations were made on the gears and the cylindrical roller bearings NJ 406.

The test conditions are given in **Table 1**. The oil temperature is set constant to 90°C and motor speed to 1500 rpm. A running-in period with 1025 N/mm^2 is set for 2 h; the test run at 1700 N/mm^2 till pitting is reached is recorded. The speed at the
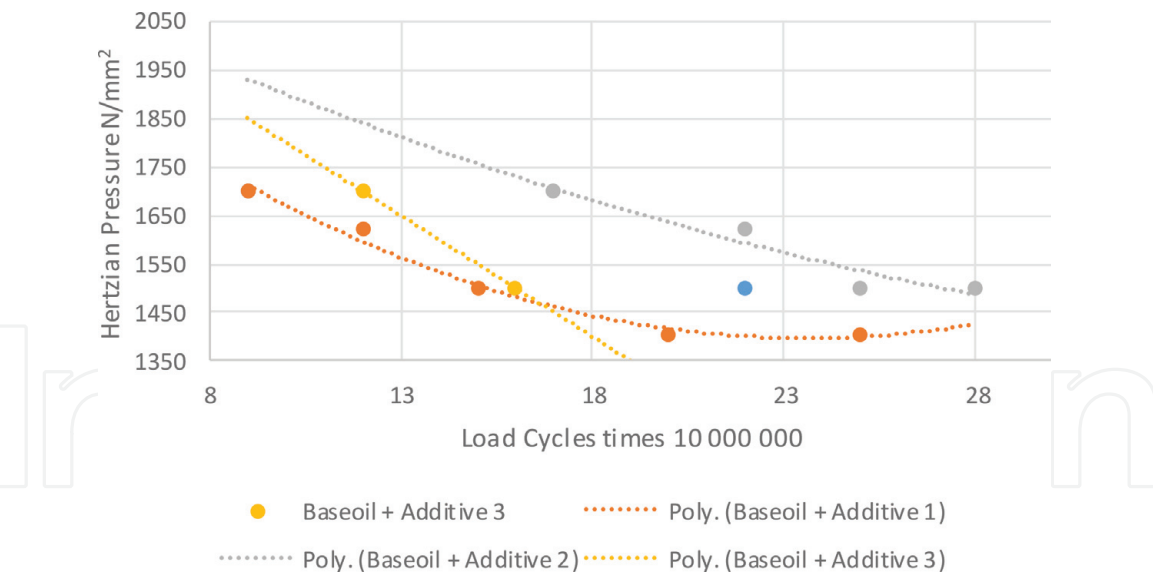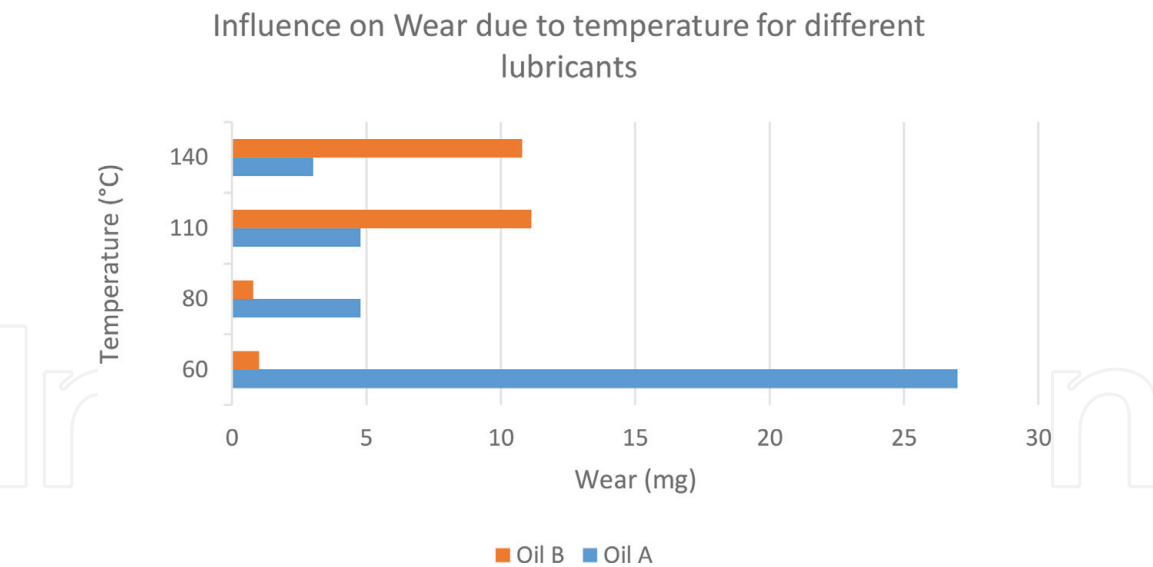
Figure 1.
The influence of different oils and additives on gear load cycles referring to the FZG test (DIN ISO 14635) [9].
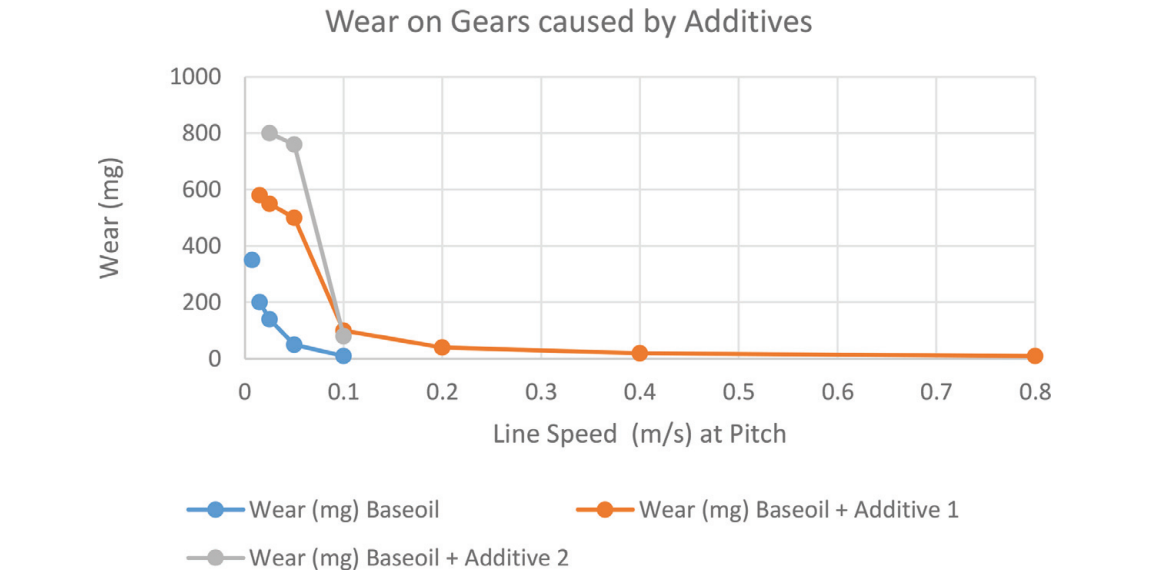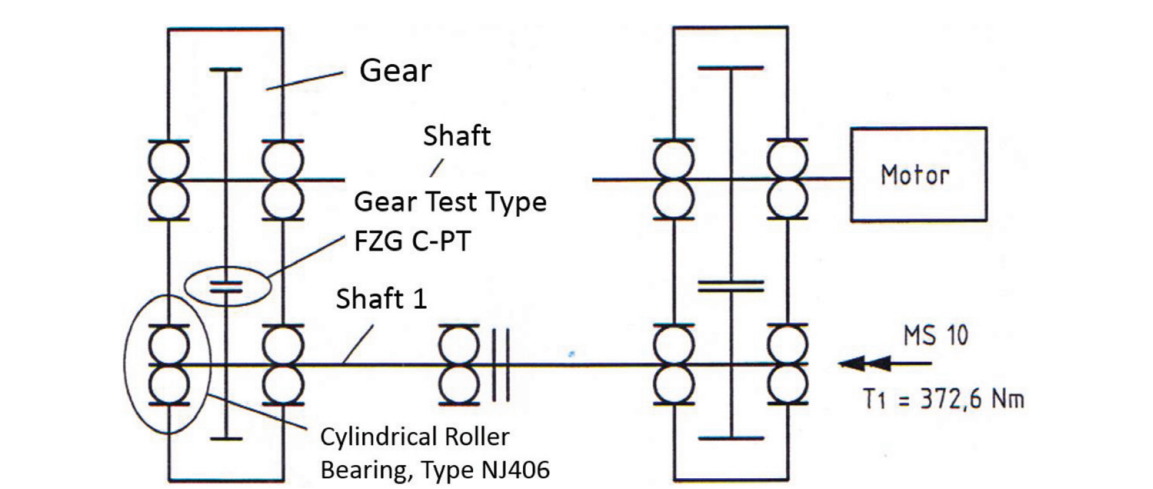

Figure 2.
Wear rate of lubricants as a function of pitch line speed.
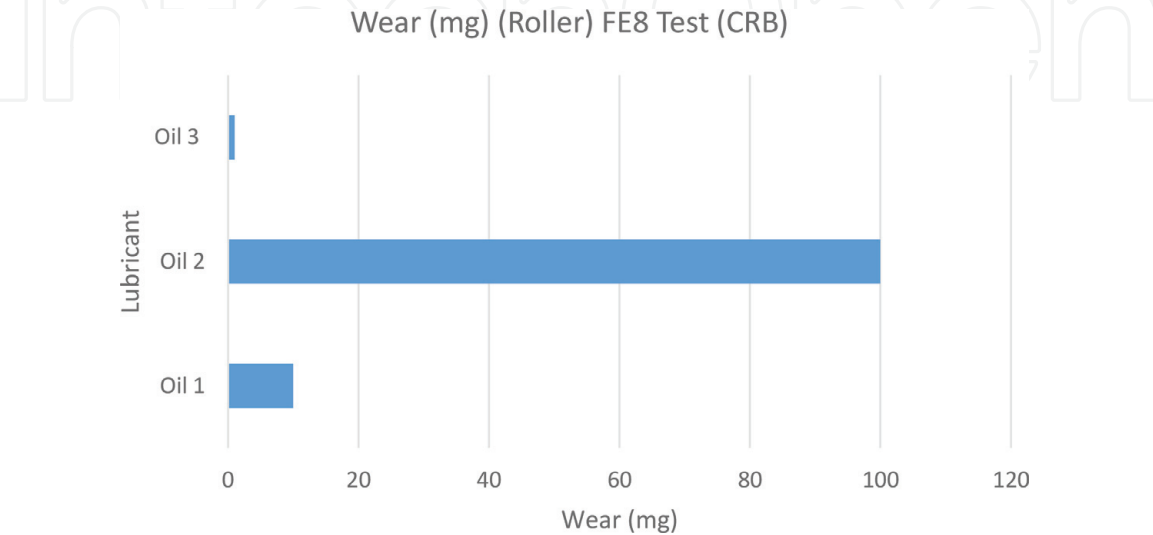
Figure 3.
Wear rate (roller) at a cylindrical roller bearing (CRB) from the Schaeffler test rig FE8 (DIN 51819) as a function of lubricants. While oil 1 and oil 3 do not show any wear, oil 2 is high in wear.

Influence on Wear due to temperature for different
lubricants

Figure 4.
Influence on wear due to temperature.

Figure 5.
FZG test rig (DIN ISO 14635).

Oiltemperature	90°C
Motor Speed	1500rpm
Running -in	1025 N/mm² for 2 hours
Test Run	1700 N/mm2
End of Test	Pitting, maximum 300 hours
Speed at the pinion	2250 rpm
Torque moment at the pinion	372,6 Nm
Type of Lubrication	Sump
Tagential Speed at the pinion	2.42 m/s
Tangential Speed at the wheel	3.87 m/s
Sliding speed at the pinion	-1.45 m/s
Sliding speed at the wheel	1.45 m/s
Sum of Speed	6.29 m/s

Table 1.
Conditions of the test.

pinion is set to 2250 rpm, the torque moment T1 to 372.6 Nm. The tangential speed at the pinion is calculated to 2.42 m/s, at the wheel to 3.87 m/s, the sliding speed at the pinion to −1.45 m/s (reflecting the negative slip), the sliding speed at the wheel

to 1.45 m/s, and the sum of speed to 6.29 m/s. As the slip percentage is given by the ratio of sliding speed to the sum of the speed, the slip at the pinion is −23% and at the wheel +23%.

The material of the gears applies for a case-hardener SAE 4320.

The test specific data of the CRB NJ206 are given in **Table 2**.

The material of the bearing accords to the *SAE 52100*, martensitic hardening, tempered at 180°C, 2 hours, with 10–12% retained austenite.

Two lubricants were tested (**Table 3**). *Lubricant 1* reflects a standard technology, using zincdithiophosphates (C4ZndtP) as a sulfur-phosphorus carrier. As a representative of a new ashless additive technology, the *lubricant formulation 2* (C4NdtP) is used. The Poly-α-olefine viscosity is 46 mm^2/s at 40°C.

The organic chain length of the phosphorus-sulfur core is given by four C atoms, meaning that during the synthesis of the additives, a C4 (butyl) alcohol component was used.

The structure of the additives are shown in **Figures 6** and 7, both looking rather complex. In detail a core of sulfur, phosphorus, and zinc is attached to the carbon sites, containing four C atoms (ZndtPC4) (**Figure 6**).

Figure 7 represents the C4NdtP; two structures are held together by an ionic bonding: a sulfur-phosphorus component with two carbon sites, each containing four C atoms and their attached hydrogen and nitrogen component with a positively charged nitrogen at the edge, attached to a carbon site with eight C atoms (C4NdtP). The principal of this substance is similar to ionic liquids, where opposite-charged atoms create an ionic binding, while the carbon sites are responsible for the liquid structure.

The test runs by the use of the different additives are given in **Table 4** for both gears and bearings (NJ406) as a function of the load cycles. Clearly the table shows how the change in the chemical structure of the additive, despite the same chain lengths on the carbon edge (C4), end up in different load cycles (**Table 4**):

| Position	Value
Innerdiameter	30 mm
Outerdiameter	90 mm
Width	23 mm
Diameter of the rollers	14 mm
Length of the rollers	11.6 mm
Curvature at Inner Race	22.5 mm
Curvature at Outer Race	-36.5 mm
Number of Rollers	9

Table 2.
Data from the CRB NJ206 bearing.

1	Poly-α-Olefine, ISO VG 46	99.29	%
	Zincdithiophosphate C4	0.71	%
2	Poly-α-Olefine, ISO VG 46	99.17	
	Ammoniumdithiophosphate C4	0.83	%

Table 3.
Lubricants used for the test.
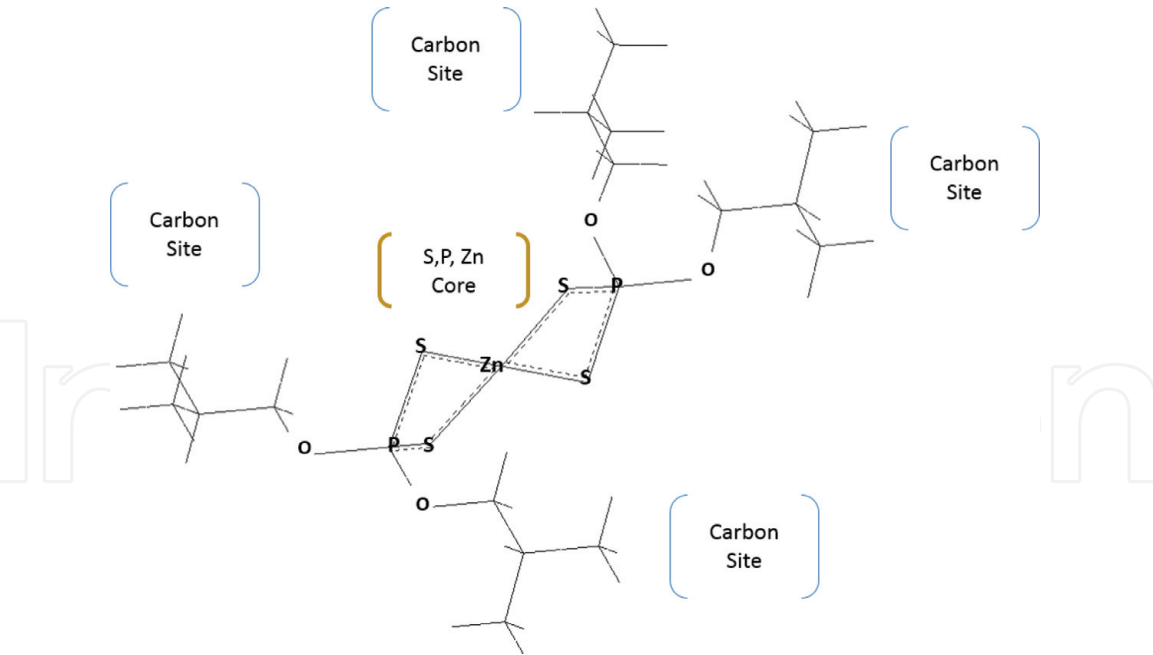
Figure 6.
Zincalkyldithiophosphate (C4ZndtP).
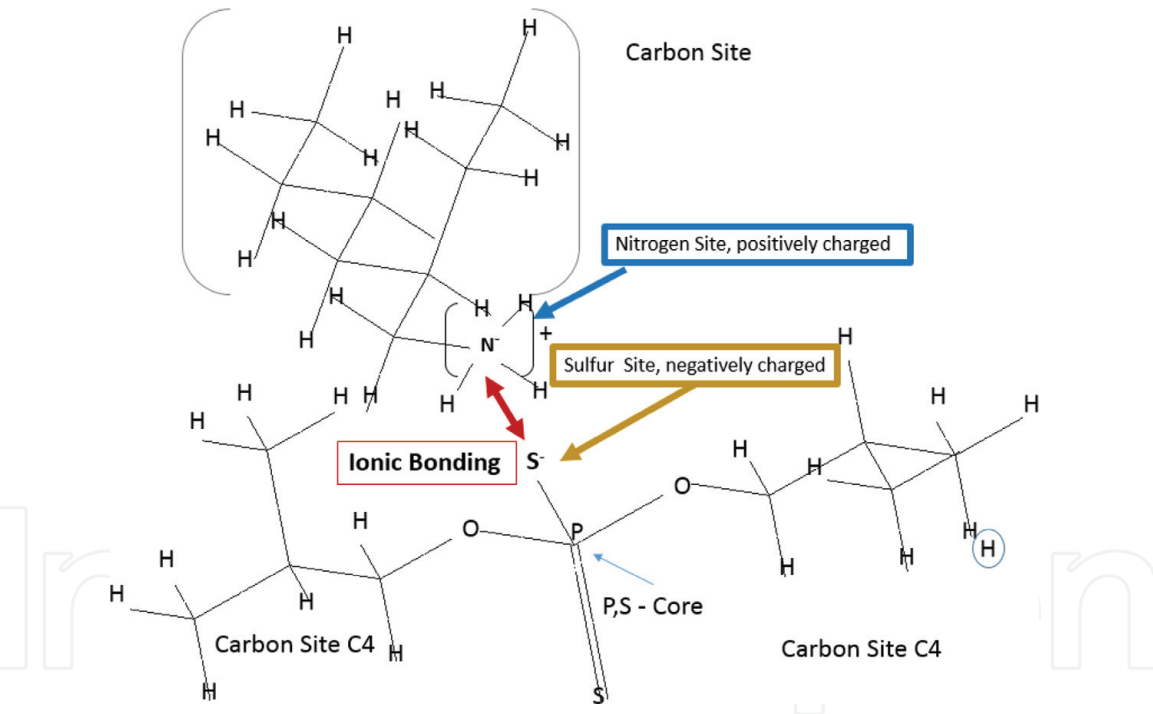
Figure 7.
*Ammoniumdithiophosphate (C4NdtP) as an ionic liquid-like structure.*

Run Nr	Component	Baseoil	Additive	Amount (%)	Temperature (°C)	Load Cycles(10^6)
1	Gear	Poly-α-Olefine, ISO VG 46	ZndtPC4	0.71	90	9.31
2	Gear	Poly-α-Olefine, ISO VG 46	ZndtPC4	0.71	90	7.8
3	Bearing	Poly-α-Olefine, ISO VG 46	ZndtPC4	0.71	90	
4	Gear	Poly-α-Olefine, ISO VG 46	NdtPC4	0.83	90	16.29
5	Gear	Poly-α-Olefine, ISO VG 46	NdtPC4	0.83	90	12.71
6	Bearing	Poly-α-Olefine, ISO VG 46	NdtPC4	0.83	90	

Table 4.
*Test conditions set on the different additive structures.*

3. Results for the gear

While the C4-Zincalkyldithiophosphate (C4ZndtP) causes pitting and does not meet the expected load cycles, the test carried out with the C4NdtP was out of failure [7]. Secondary neutral mass spectrometry (SNMS) profiles [21–23] were carried out at the pinion *addendum* (*Position 1*: see arrow in **Figure 8**) (area of *positive* slip referring to the pinion), the *pitch line* (*Position 2*: see arrow in **Figure 8**) (*zero slip* referring to the pinion), and tooth *dedendum* (*Position 3*: see arrow in **Figure 8**) (area of *negative slip*) in order to evaluate how the reaction rate of additives might depend on load cycles. The nature of the reaction was analyzed by secondary neutral mass spectrometry (SNMS). While secondary ion mass spectrometry (SIMS) is sensitive due to the local elements, specifically oxygen, SNMS is less sensitive and allows to track elements quantitatively as depth profiles from the top of the surface down to a few microns. The spatial resolution is around 4 mm^2, thus averaging local deviations in elements making the results more accurate.

The relevant depth profiles were taken at the dedendum of the pinion tooth flank for the additives C4-zincalkyldithiophosphate (C4ZndtP) and C4-aminealkyldithiophosphate (C4NdtP) with respect to load cycles are shown in **Figure 9** (C4ZndtP: 9×10^6 load cycles); **Figure 10** (C4ZndtP: 10×10^{10} load cycles); **Figure 11** (C4NdtP: 12×10^6 load cycles); and **Figure 12** (C4ZndtP: 16×10^{10} load cycles).
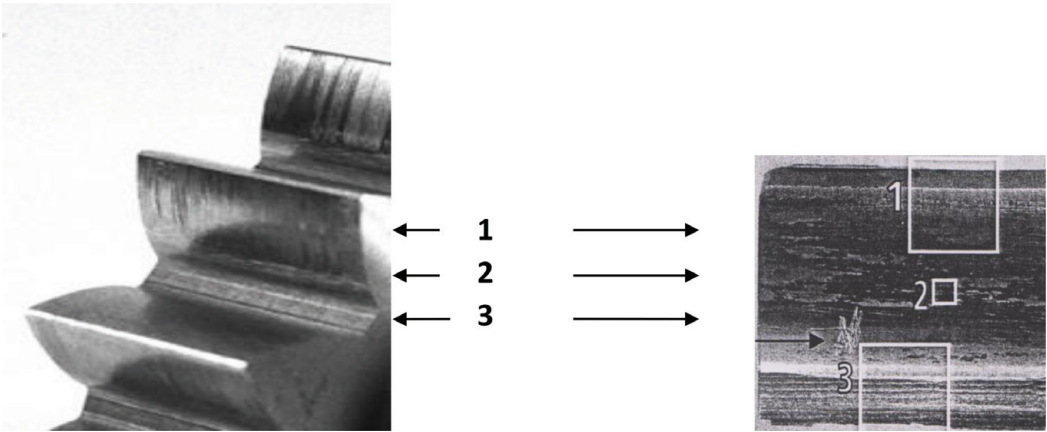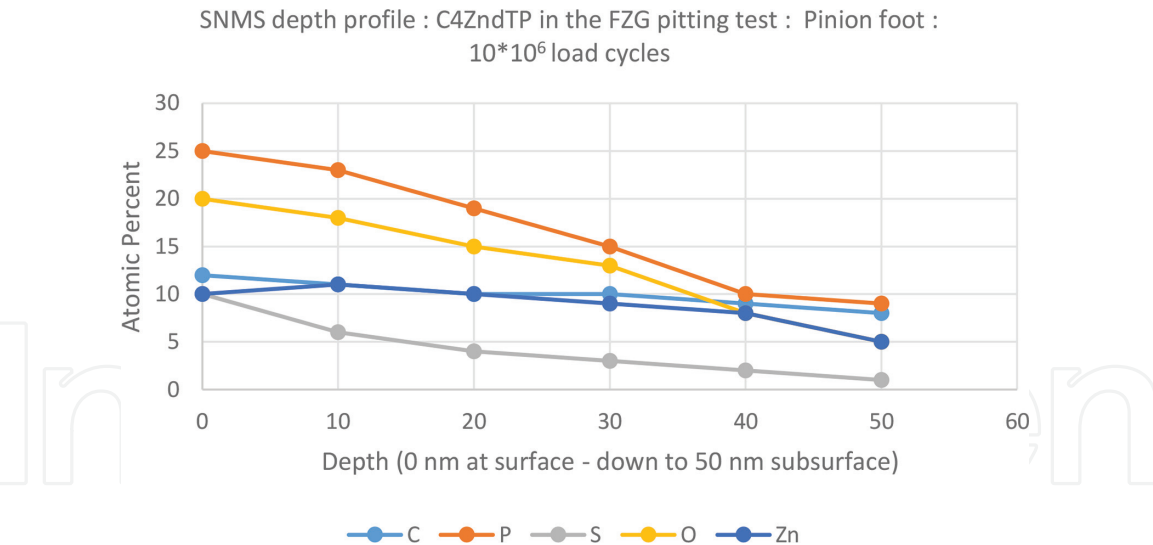

Figure 8.
Gear tooth segment with addendum Position 1 (pitch line), Position 2, and Position 3 as dedendum.
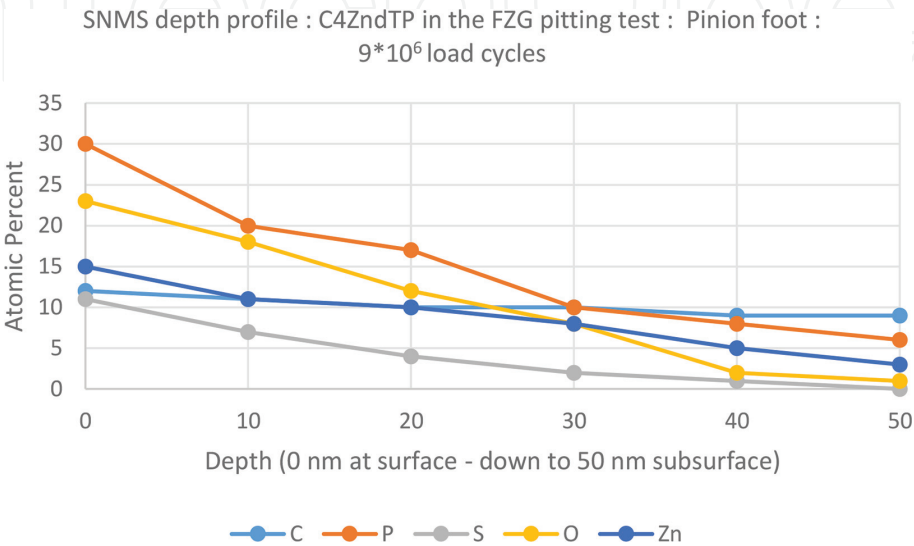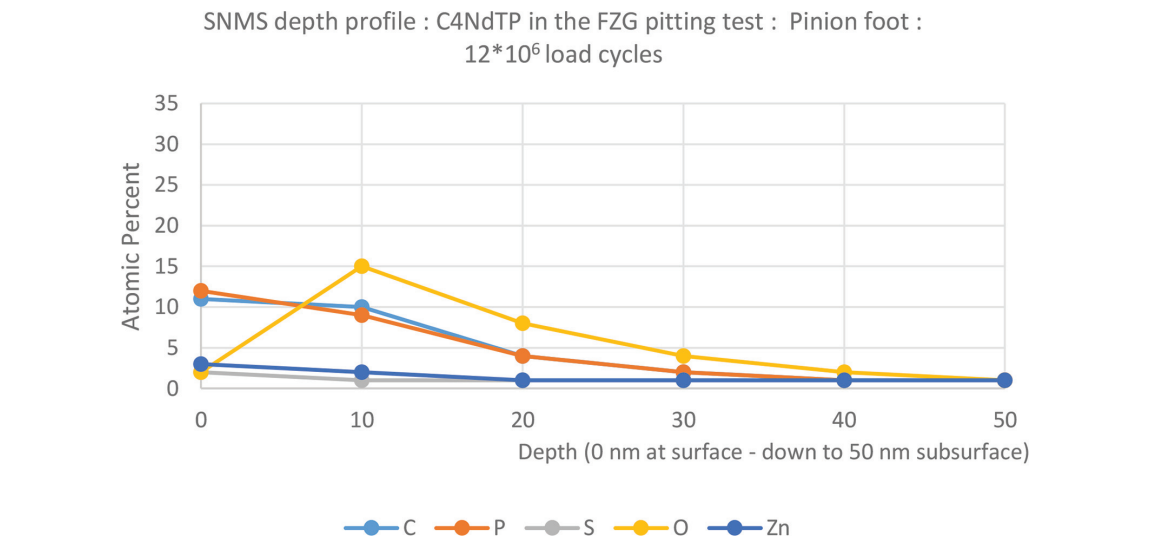

Figure 9.
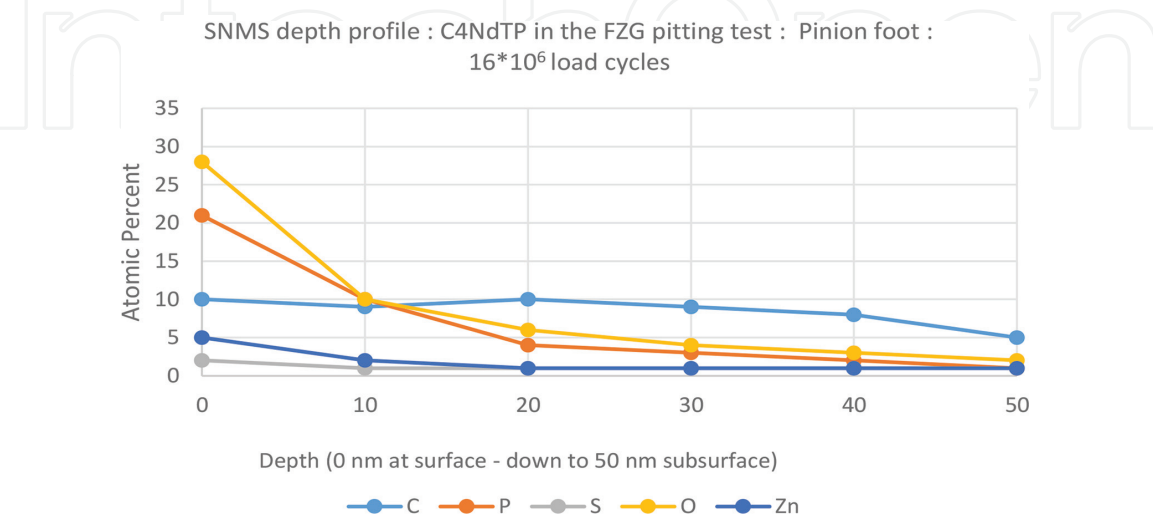*SNMS depth profile: C4ZndtP in FZG pitting test at 9×10^6 load cycles.*

Figure 10.
SNMS depth profile: C4ZndtP in FZG pitting test at 10×10^6 load cycles.

Figure 11.
SNMS depth profile: C4NdtP in FZG pitting test at 12×10^6 load cycles.

Figure 12.
SNMS depth profile: C4NdtP in FZG pitting test at 16×10^6 load cycles.

8

As a result from *A1–A2*, C4ZndTP causes pitting and increases in layer thickness formation, while *B1–B2* C4NdtP does not at prolong load cycles however shows an increase in surface reaction of the phosphorus component while the reaction layer stays constant.

4. Results for the bearing (NJ406)

The calculation of the load distribution is shown in **Table 5** and **Figure 13**.

The maximum force is acting on roller nr. 7 with a contact pressure of 1481 N/mm^2 [7].

The results (see **Figures 14** and **15**) show an impact of zinc, assumed to be a mixture of phosphates and zinc oxide in the case of the C4ZndtP at 19×10^6 load cycles (**Figure 14**), while compared with the oxygen in the case of the C4NdtP stays low (**Figure 15**).

The bearing thus gives a different reaction by embedding zinc oxide in the near surface. The results for the C4NdtP are quite similar to the reactions seen in the gear.

|	
Speed of the Innerring	2250 m/s
Speed of the Cage	858 m/s
Speed of the Rollers	- 4474 m/s
Tangential Speed at the Inner Ring Raceway	3.28 m/s
Tangential Speed at the Rollers	3.28 m/s
Sum of Speed	6.56 m/s
Pressure at Roller Nr 7 versus Innerring	1481 N/mm^2

Table 5.
Conditions at the bearing NJ406.
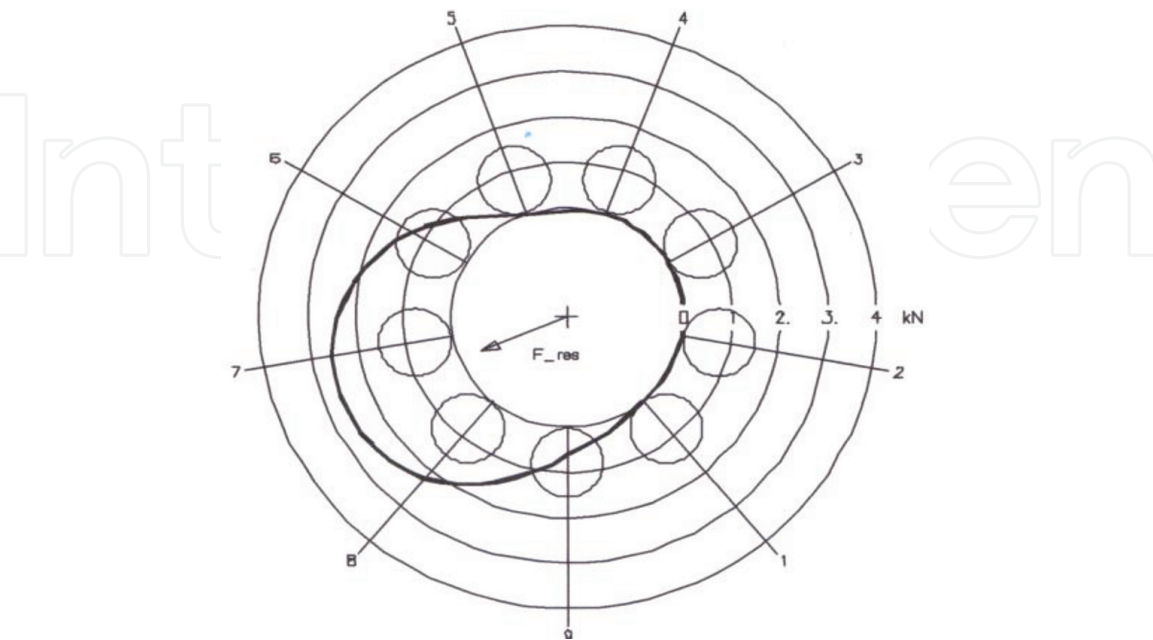
Figure 13.
Load distribution for the NJ406 bearing.
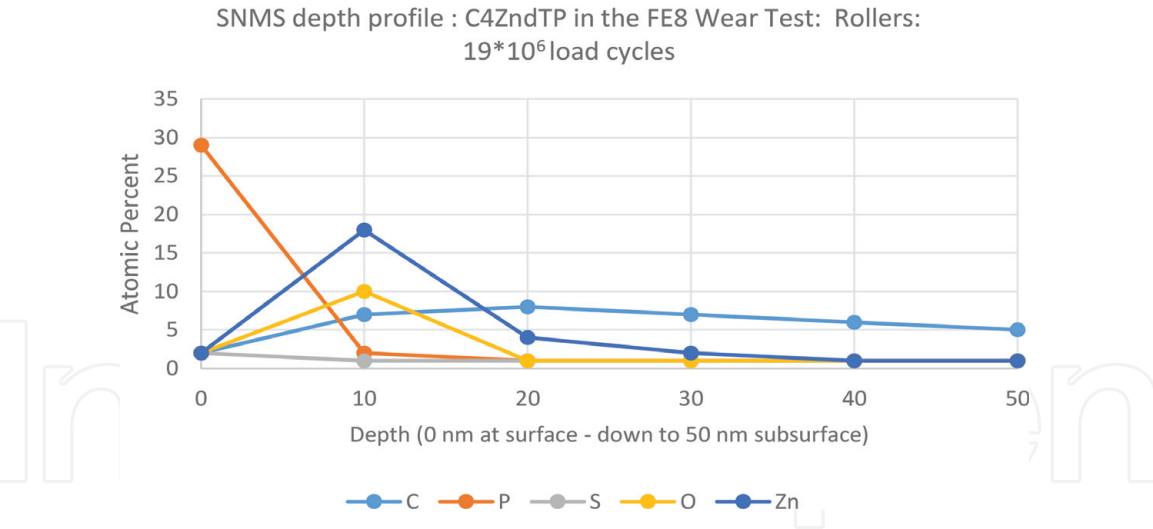
Figure 14.
SNMS depth profile: rollers, C4ZndtP in FE8 bearing test at 19×10^6 load cycles.
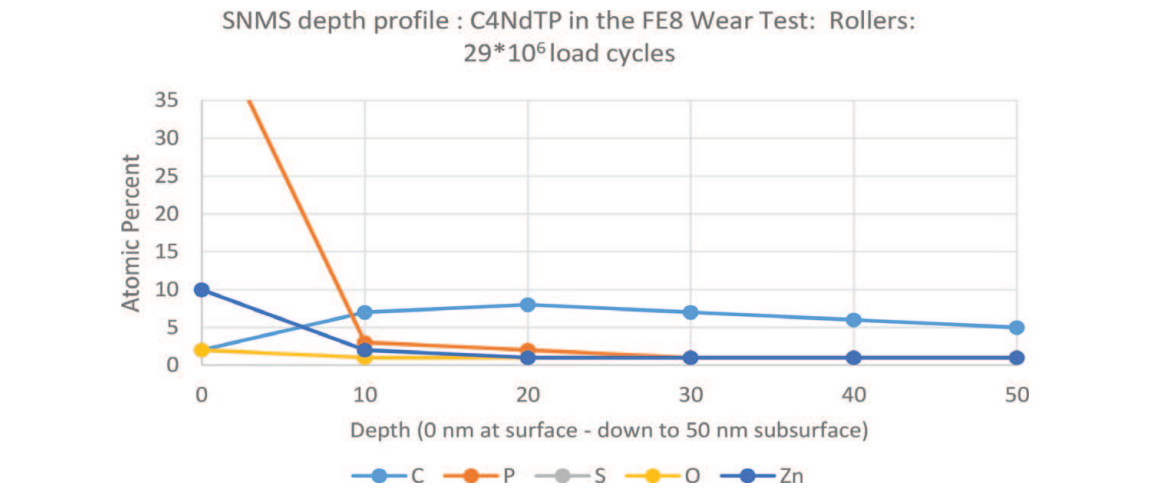
Figure 15.
SNMS depth profile: C4NdtP in the FE8 wear test, rollers at 29×10^6 load cycles.

5. Gear: reaction rates

For the gear (pinion, dedendum) the reaction turnover stays constant or slightly decreases for the C4ZndtP (**Figure 16**) but increases in depth by the use of C4NdTP (**Figure 17**).

The reaction film thickness shows a progression in the case for the C4ZndtP (**Figure 18**), while the C4NdtP shows a regression in time (**Figure 19**).

## 6. Gear: nanohardness measurement at the pinion

Nanohardness measurements are shown in **Figures 20–22**: **Figure 20** shows the as-received hardness profile of the dedendum, pitch, and addendum for the as-received pinion tooth flank material (case-hardener SAE 4320).

Figure 21 shows a *steep decrease* by the use of the C4ZndtP compared to the as-received material at the surface.

Figure 22 shows a *steep increase* by the use of C4NdtP compared to the as-received material at the surface.
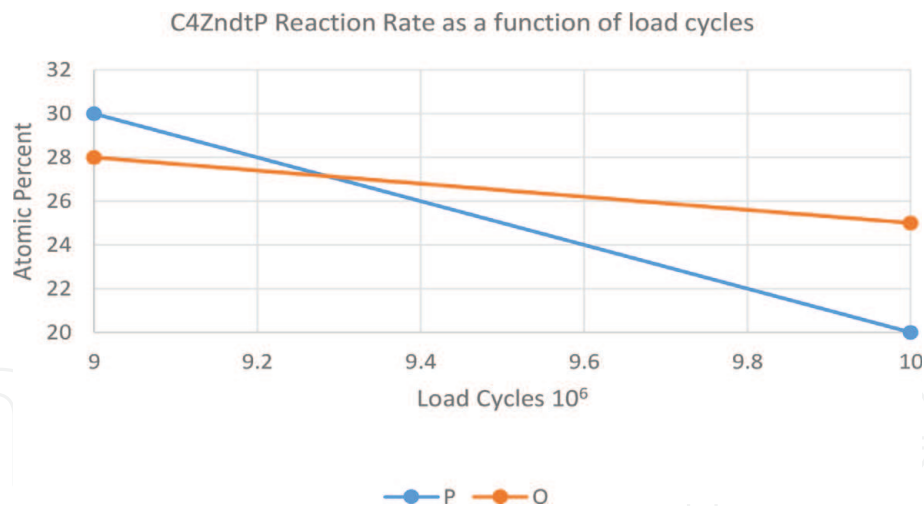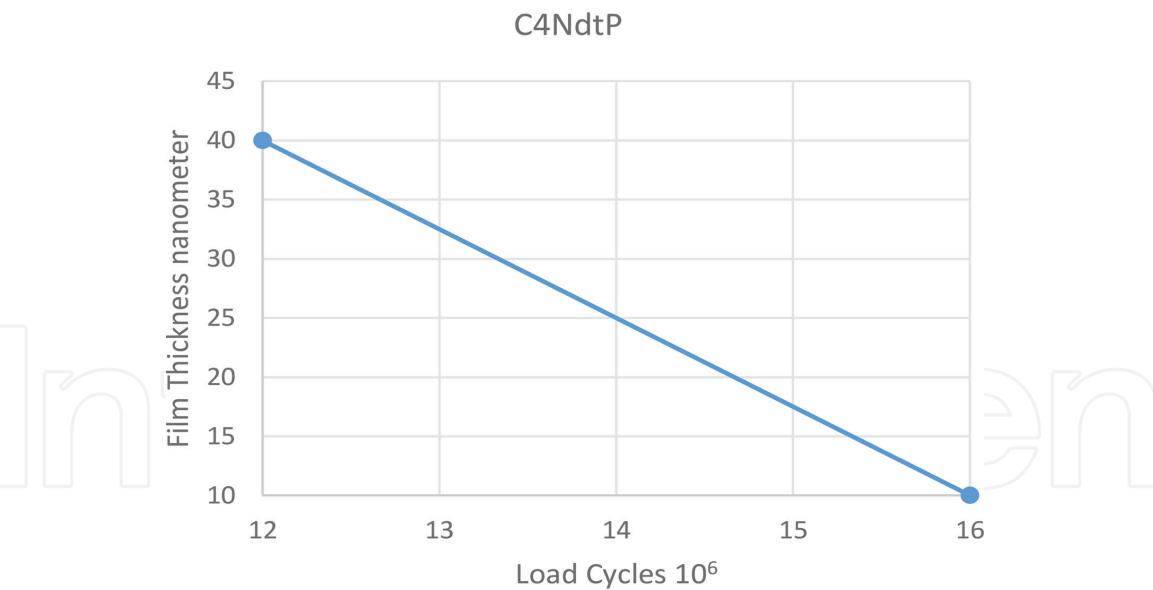
Figure 16.
SNMS profiles: reaction rate (elements phosphorus and oxygen) in the FZG gear tests for C4ZndtP as a function of load cycles.
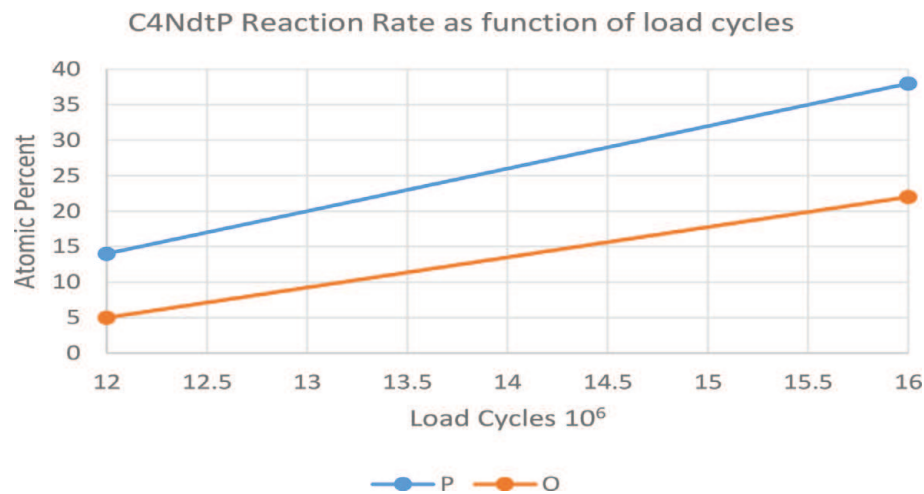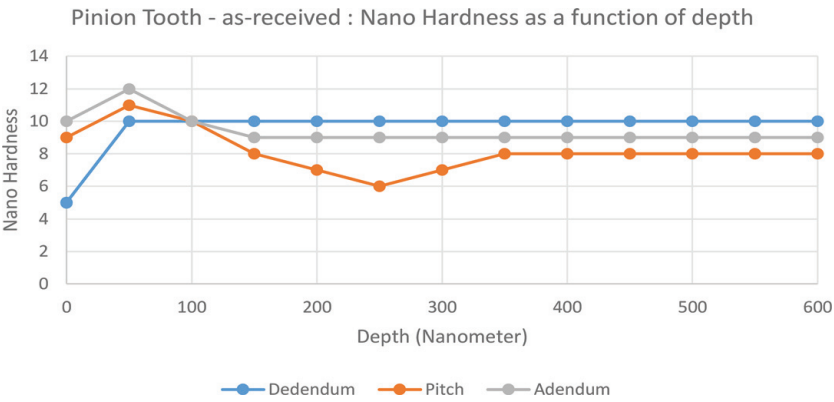

Figure 17.
SNMS profiles: reaction rate (elements phosphorus and oxygen) in the FZG gear test for C4NdtP as a function of load cycles.
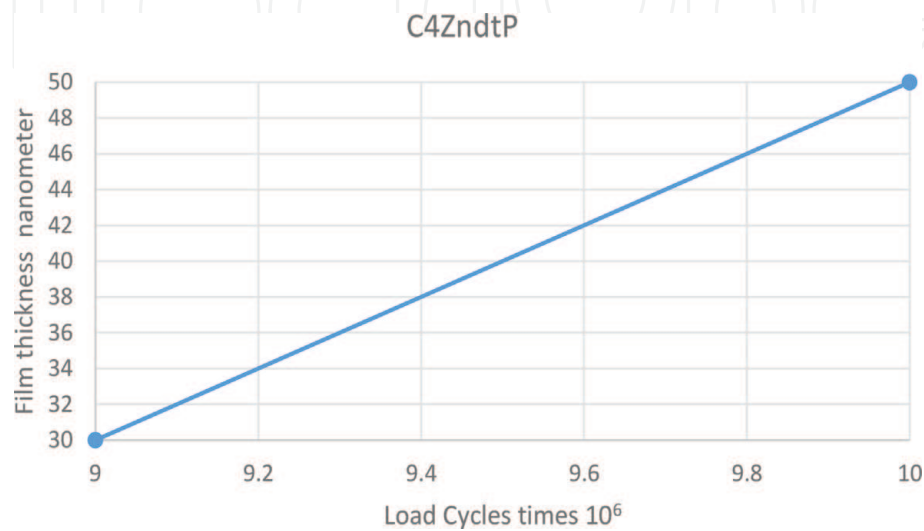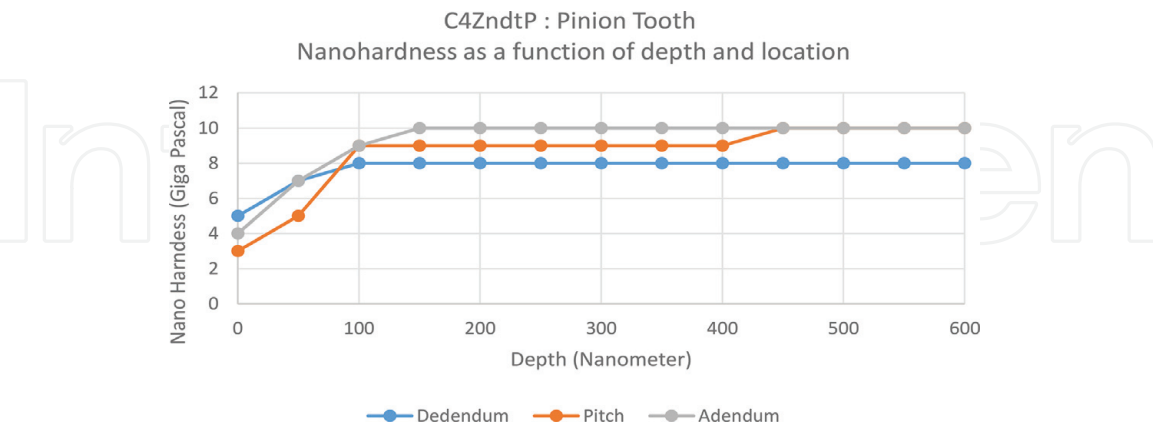

Figure 18.
C4ZndtP: process of film thickness formation as a matter of load cycles.

11

Figure 19.
C4NdtP: process of film thickness formation as a matter of load cycles.

Figure 20.
Nanohardness measurements for the as-received pinion (from dedendum via pitch to the addendum).

Figure 21.
C4ZndtP: pinion tooth nanohardness as a function of depth (nanometer) and location (dedendum, pitch, and addendum).

7. Molecular description

As functional groups in additives determine the reliability of drivetrain components, it is of interest how those processes are to interpret. Coming from the molecular perspective with a size of 10^{-9} m, it takes effort to interpret effects
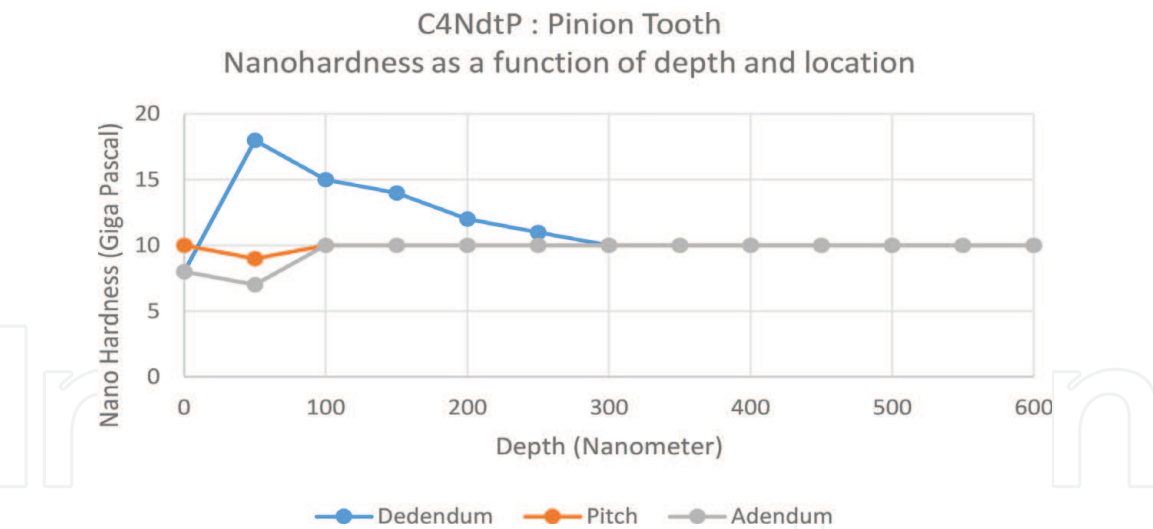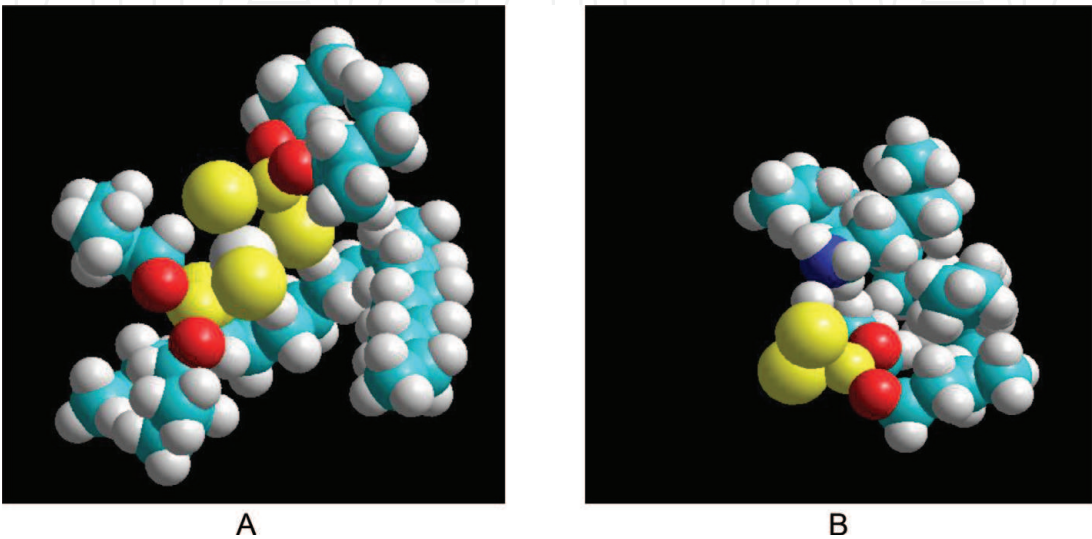
Figure 22.
C4NdtP: pinion tooth nanohardness as a function of depth (nanometer) and location (dedendum, pitch, and addendum).

on 10^{-9} till 10^{-3} m, e.g., magnitudes of 10^6 in length scale. However, considerable progress in multi-scale modeling has become real in the last years; it is of interest how to predict the observed effects reported here by the use of predictors. Basically predicators are obtained by the properties of a molecule, e.g., coming from the chemical bonding. Exploring molecules by quantitative structure property relationship (QSPR) [24] and the molecular properties by the use of density functional theory (DFT) is a standard [25]. The interaction of molecules with themselves and with surfaces is part of molecular dynamics and ab initio methods.

Figure 24A and **B** shows the surface of the additive C4ZndtP with one molecule PAO (as a hydrogenated Di-Dec-1-ene, $C_{20}H_{42}$) (A) and the additive C4NdtP with one molecule PAO (as a hydrogenated Di-Dec-1-ene, $C_{20}H_{42}$) (B) energy minimized by the use of molecular dynamics.

Figure 24A shows the surface of the additive C4ZndtP with one molecule PAO (as a hydrogenated Di-Dec-1-ene, $C_{20}H_{42}$) and the additive C4NdtP with one molecule PAO (as a hydrogenated Di-Dec-1-ene, $C_{20}H_{42}$) (B) attached to an ideal body-centered cubic (bcc) iron surface as C for the C4ZndtP and D for the C4NdtP, energy minimized by the use of molecular dynamics.

Figure 23.
(A) C4ZndtP structure in PAO and (B) C4NdtP structure in PAO.
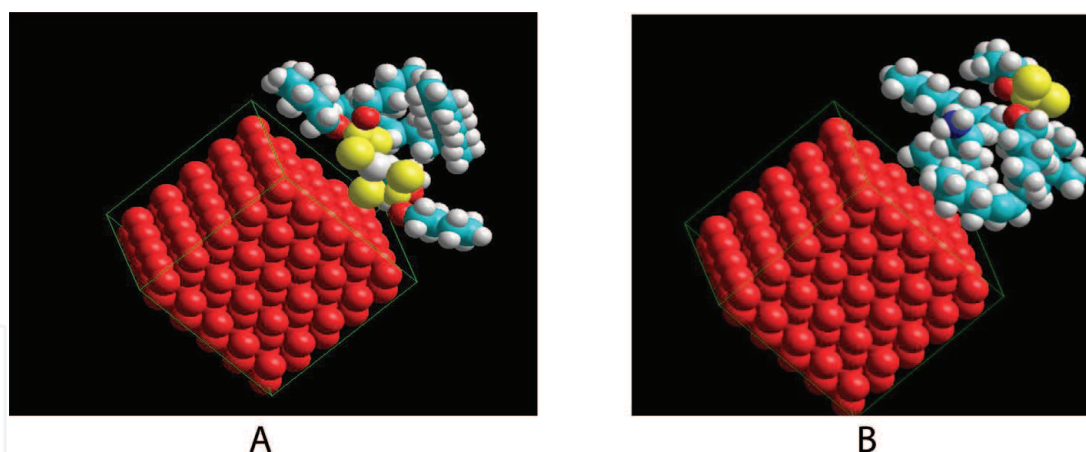
Figure 24.
(A) Approaching a (A) C4ZndtP and (B) C4NdtP to an ideal bcc, iron surface. Labeled atoms are: red: iron; dark red: oxygen; blue: carbon; gray: hydrogen; and yellow: sulfur.

Figure 23B shows the surface of the additive C4ZndtP with one molecule PAO (as a hydrogenated Di-Dec-1-ene, $C_{20}H_{42}$), and the additive C4NdtP with one molecule PAO (as a hydrogenated Di-Dec-1-ene, $C_{20}H_{42}$) (B) attached to an ideal body-centered cubic (bcc) iron surface as C for the C4ZndtP and D for the C4NdtP, energy minimized by the use of molecular dynamics. Approaching this system to an ideal iron surface, it is obvious that the C4Zn is attached with the polar edge (Zn, P, S) to the surface (see **Figure 24A**), while the C4NdtP is attached via the carbon shell (see **Figure 24B**).

8. Discussion

The results shown here may give a reasoning about the elementary analyses found by SNMS where the C4ZndtP progressively acts in time by increasing the reaction layers toward 50 nm constituted by P, O, and Zn oxides, while the C4NdtP shows an initial reaction in the beginning, but regressing the layer to a constant film at 10 nm [26].

As for the C4ZndtP, the reactive core is near to the surface; the reaction may proceed by continuous load cycling, which is found in the SNMS profiles. Due to the continuous degression of the surface toward oxides, the C4ZndtP shows a decrease in the nanohardness by the fact that the surface gets covered with material softer than the base. Also the reaction rate goes down due to fact that the reaction layers are chemically inert compared to iron. The remote position of the reactive group in the C4NdtP exposes the sulfur-phosphorus core to the environment as oxygen. Tribological impacting may then promote the oxidation of the reactive site, rather than a reaction with the metal surface. This means that in the first step the C4NdtP reacts with oxygen at the reactive site, coming to phosphoric acid specie. Those would turn to the surface as they are not soluble in the base oil and naturally get attracted by the oxide sites at the metal surface. The amine would be dissolved back into the base oil. As a fact those phosphoric acid specie are found to be detached on the surface of the pinion dedendum. The oxidation will continue; hence, it is expected that the phosphorus-oxide layer will increase on top, but no material will be leached out due to the fact that the phosphates and polyphosphates are uniquely covering the surface, not being soluble in the matrix.

While the C4ZndtP obviously causes a successive exchange of near-surface material (e.g., iron), the C4NdtP does not. The hardness profiles might be coherent with the carbon profile (SNMS): while the C4ZndtP converts constantly the surface

material by smooth oxides, the C4NdtP creates a thin phosphorus-oxide layer on top on a size of 10 nm. The carbon site exposed to the metal might protect it against oxidation, and as the reactive phosphorus-sulfur site is remote, the hardness at least does not go down. The steep increase could be caused by a hardening process of the surface due to carbide formation at the interface as a degradation process of the carbon site. It is noteworthy to say that this interpretation is related to the positions of negative slip and speculative.

Hence, the structure of an additive determines how it approaches and how the subsequent reactions take place, either on the site of the functional head or on the site of the carbon, ending up in the reliability of the application with respect to pitting.

9. Conclusions

The reliability of drivetrain with respect to its expected life cycle is of key interest in the value chain of an installation. Each component contributes to this by the matter of load impacting the load capacity of the materials involved. As load capacity is well defined for the construction materials, e.g., gears and bearings, this definition becomes vague for lubricants. Even though a malfunction of a lubricant could cause damage features, like wear, friction, and tribocorrosion, the under-standing of the real function and how to judge it by robust predictors is still missing. Lubricants may give malfunction even in the case of a proper application due to the interaction of functional additives with the mating surfaces. Plenty of contributions worldwide show that the "construction" of a lubricant by adding functional addi-tives into a base oil may lead to premature failures given by the interaction of the functional additives with the given surface. Normally additives are readily dissolved in a base oil and as such transported to the points of interacting surfaces, there getting released in order to uptake a function like wear prevention or friction reduction. However, the energy offered by the contact due to sliding and contact pressure makes additives reactive, causing chemical reactions. The chemical reac-tions with different additives are seen by the use of specific test conditions, presented in the study as an FZG back-to-back gear test rig. The study brings out that a traditional anti-wear additive such as a zincdithiophosphate (C4ZndtP) reacts continuously at a given threshold with the surface, exchanging the near-surface material. The softening causes continuously material loss over time, ending up in pitting. In contrast, just by changing the chemical structure from a zincdithiophosphate to an ionic liquid like amine-neutralized dithiophosphate (C4NdtP); it is obvious that the application fulfills the complete life cycle without pitting. Compared to the zincdithiophosphate (C4ZndtP), it comes out that the amine-neutralized dithiophosphate (C4NdtP) hardens up at the area of negative slip at the pinion dedendum. Technical data are not to explain this elementary topic. Hence, it has to be seen in a deeper aspect. As additives are dissolved readily in the base oil, the tribological process makes them approach the surface. This brings up the question how the additive is released from the base oil toward the surface as the initial step. In the given example, a simple molecular model shows that in the case of the zincdithiophosphate, the additive approaches the surface with the reactive site given by the sulfur and phosphorus core, continuously leaching iron out of the surface with a subsequent weakening created by reaction layers with little binding to the core of the material. In the case of ammonium-neutralized dithiophosphate, the molecular model shows that this additive approaches the surface by the carbon site, while the sulfur-phosphorus site is remote. This additive gives a hardness increase during the tribological interaction, and as a speculation, the tribological

energy may crack the molecule to carbon specie, subsequently hardening the surface up by carbides and preventing an excessive penetration of reaction products.

10. Summary

Additives are part of a drivetrain reliability. It comes clearly that within a construction, the tribological energy offered by the kinematics, the surrounding temperature and environment plus the material involved, has to be judged in terms of the structure of lubricants in the molecular level and how those structures compete with the offer of tribological energy.

Starting from a very basic and standard molecular model, it is essential to understand how additives dissolve in a base oil and how they get released and redissolved at a tribological contact area. Even though how additives act toward a surface might be a minor question, it turns out to be very essential and at least the limiting factor of an application reliability if the criticality of those processes are unknown and might pop up in a given application as premature failure.

Abbreviations

C4ZndtP	isobutyl-zincdithiophosphate
C4NdtP	isobutyl-dithiophosphoric acid reacted with an alkylamine
FZG	gear test rig (DIN ISO 14635)
FE8	bearing test rig (DIN 51819)
PAO	poly-α-olefine as a hydrogenated poly-dec-1-ene
SNMS	secondary neutral mass spectrometry
CRB	cylindrical roller bearing
bcc	body-centered cubic
MPa	megapascal (10^6 Pa)

Author details

Walter Holweger[1,2]

1 Technological Consultant Agency, Epfendorf, Germany

2 Schaeffler Technologies AG & Co. KG, Herzogenaurach, Germany

*Address all correspondence to: walter.holweger@t-online.de

IntechOpen

References

[1] Kragelski IV, Dobycin MN, Kombalov VS. Grundlagen der Berechnung von Reibung und Verschleiß. München, Wien: Carl Hanser Verlag; 1982. ISBN: 3-446-13619-3

[2] Bowden T. Friction and Lubrication of Solids. Oxford/Berlin: Clarendon Press/Springer; 1950. ISBN: 978-3-642-92755-3

[3] Zum Gahr K-H. Microstructure and Wear of Materials. Amsterdam: Elsevier; 1987. ISBN: 0-444-42754-6

[4] Rabinowitcz E. Friction and Wear of Materials. New York: Wiley-Interscience; 1995. ISB-0-471-83084-4

[5] Czichos H, Habig K-H. Tribologie-Handbuch. Wiesbaden: Vieweg & Teubner; 2010. ISBN: 978-3-83480-017-6

[6] Bushan B. Modern Tribology Handbook, Vol. 1(2). New York: CRC Press; 2001

[7] FVA Report, 289 I & II. Zusammenhänge zwischen Zahnrad- und Wälzlagerschäden und tribologischen Veränderungen des oberflächennahen Werkstoffbereichs; 2001–2003

[8] Johanssen J. On the Influence of Gear Oil Properties on Pitting Life. Lulea: University of Lulea; 2015

[9] FZG Test Rig. Available from: https://www.researchgate.net/publication/235308055_Testing_procedures_for_gear_lubricants_with_the_FZG_test_rig

[10] Geheeb N, Franke J. Forschungsvereinigung Antriebstechnik. FVA 126. RWTH Aachen: Vogel Verlag; 2000

[11] Reichelt M. Mikroanalytische Klärung Des Verschleißschutzes in Langsam Laufenden Wälzlagern. Aachen: Shaker; 2011. ISBN: 978-3-8440-0424-3; ISSN: 1618-5722

[12] Höhn BR, Oster P. Influence of the Lubricants on Pitting and Micro Pitting in the FZG Gear Test Rig. Hamburg: Deutsche Wissenschaftliche Gesellschaft für Erdöl, Erdgas und Kohle e.V.; 1996

[13] Winter H, Michaelis K. AGMA Technical Paper P291.17, scoring load capacity of gears lubricated with EP-oils. In: Fall Technical Meeting; October 17–19; Montreal, Canada; 1983

[14] Schönnenbeck G et al. Mineralöltechnik. 1987;**32**(6):1-24

[15] Vinogradova IE. Antianrißinhibitoren für Öle. Moskau: Verlag Chimija; 1972. p. 272

[16] Ruina A, Pratap R. Introduction to Statics and Dynamics. Oxford: Oxford University Press; 2002. p. 713

[17] Arun AP, Senthil AP, Giriaj B, Faizur RA. Gear test rig—A review. International Journal of Mechanical & Mechatronics Engineering. 2014;**14**. No: 05 16 140205-9696-IJMME-IJENS ©

[18] Hibbeler RC. Engineering Mechanics. 11th ed. New Jersey: Pearson/Prentice Hall; 2007. p. 393. ISBN: 0-13-127146-6

[19] Castro J, Sottomayor A, Seabra J. Experimentals and analytical scuffing criteria for FZG gears. Tribology Series. 2003;**43**:651-661

[20] Fernandes C, Blazquez L. FZG gearboxes lubricated with different formulations of polyalphaolefin wind

turbine gear box oils. In: International Gear Conference, Lyon; 2014

[21] Jede RH, Peters RH, et al. Analyse dünner Schichten mittels Massenspektrometrie zerstäubter Neutralteilchen. TM—Technisches Messen. 1986;**11**:407-413

[22] Passlack S, Kopnarski M. Sekundärneutralteilchen-Massenspektrometrie (SNMS). 2014. Available from: https://onlinelibrary. wiley.com/doi/pdf/10.1002/vipr. 201400569

[23] Vad K, Csik A, Langer G. Secondary neutral mass spectrometry—A powerful technique for quantitative elemental and depth profiling analyses of nanostructures. Chichester, UK: Spectroscopy Europe; 2009:13-16. Available from: https://www.spectrosc opyeurope.com/article/secondary-ne utral-mass-spectrometry-powerful-tech nique-quantitative-elemental-and-depth

[24] Katritzky AR, Lobanov VS, Karelson M. QSPR: The correlation and quantitative prediction of chemical and physical properties from structure. Chemical Society Reviews. 1995;**24**:279-287. Available from: https://pubs.rsc. org/en/content/articlelanding/1995/cs/c s9952400279

[25] Bockstedte M, Kley A, Neugebauer J, Scheffler M. Density-functional theory calculations for poly-atomic systems: Electronic structure, static and elastic properties and ab initio molecular dynamics. In: Computer Physics and Communications. Vol. 107. Amsterdam: Elsevier; pp. 187-222. Available from: https://www.sciencedirect.com/science/ article/pii/S0010465597001173

[26] Szlufarska I. Multi-scale modeling of friction and wear. In: 22nd Conference of Wear of Materials; Long Beach, California; 2018. University of Wisconsin, Key Note